Journal of
Ceramic Science
and Technology

J. Ceram. Sci. Tech., **06** [01] 9-16 (2015)
DOI: 10.4416/JCST2014-00031
available online at: http://www.ceramic-science.com

Hydrothermal Synthesis of $ZnAlGaO_4$ and the Effect of the Post-Heat Treatment on the Enhancement in Crystallinity

K. Sakoda and M. Hirano*

Department of Applied Chemistry, Faculty of Engineering, Aichi Institute of Technology, Yakusa, Toyota, 470 – 0392 Japan

received August 1, 2014; received in revised form October 31, 2014; accepted December 16, 2014

Abstract

Spinel-type nanoparticles with a $ZnAlGaO_4$ composition were directly synthesized from the aqueous precursor solutions of $ZnSO_4$, $Al(NO_3)_3$ and $Ga(NO_3)_3$ under hydrothermal conditions at 150 ~ 240 °C for 5 h in the presence of tetramethylammonium hydroxide. The resulting changes in the structure and properties of as-prepared $ZnAlGaO_4$ spinel in the course of heating in air up to 1000 °C were investigated. The cell size of the as-prepared spinel phase slightly decreased as the hydrothermal treatment temperature increased from 150 to 240 °C. The nano-sized crystallite at around 8 nm of as-prepared spinel phase formed at 180 °C was maintained up to 600 °C and grew to 44 nm as the heat-treatment temperature rose from 600 to 1000 °C. The cell size of the spinel nanoparticles slightly and gradually changed during heat treatment up to 800 °C, and it almost accorded with the ideal value reported in the reference after heat treatment higher than 800 °C. The UV-blue light emission centered at 360 nm with relatively high intensity that was observed in the as-prepared spinel under excitation at 270 nm changed depending on the heat-treatment temperature. After heating at 800 °C, the spinel showed broad-band emission centered at around 430 nm.

Keywords: Oxides, chemical synthesis, spinel, crystal structure, optical properties

I. Introduction

In recent years, much attention has been devoted to wet chemical routes to synthesize nanometer-sized crystals of inorganic materials [1]. In order to improve the performance and properties of inorganic materials, investigating their synthesis routes is one approach in addition to designing the materials based on control of their microstructures and compositions. The mild hydrothermal synthesis technique, which is one of the wet chemical routes in the category of building-up processes, is well known as being able to synthesize homogeneous nanocrystalline inorganic materials from aqueous precursor solutions at relatively low temperatures [2–5].

Zinc aluminum oxide (zinc aluminate, $ZnAl_2O_4$) and zinc gallium oxide (zinc gallate $ZnGa_2O_4$), which are representative materials of oxide spinel compounds, have attracted enormous attention as wide-band-gap semiconductors thanks to their interesting and superior properties [6]. The zinc gallate spinel possesses outstanding and excellent characteristics such as being potentially transparent and conductive in the near-UV region [7]. It shows a blue emission without any dopant via a self-activation center of Ga-O groups under excitation by both UV light and low-voltage electrons [8] and shows emissions from green to red when it is doped with Cr and Mn [9]. Zinc gallate has been applied in many uses, e.g. transparent electrodes, phosphors in vacuum florescent displays [8, 10], field emission displays [11], thin film electroluminescence displays [12], and photocatalysts for the decomposition of benzene [13]. As in the case of zinc aluminate spinel, it also exhibits excellent properties such as thermo-mechanical resistance, chemical stability, high thermal stability, and photoluminescence [14, 15]. Many applications of $ZnAl_2O_4$ as reflective optical coatings [16], UV-transport electro conductive oxides [17], and photocatalysts for the degradation of toluene [18] have been reported. The main applications of $ZnAl_2O_4$ are as catalysts for dehydration [19], hydrogenation [20], dehydrogenation [21], and synthesis of fine chemicals [22]. Although many studies on $ZnGa_2O_4$ and $ZnAl_2O_4$ spinel compounds have been reported, there are only few studies on $ZnAlGaO_4$ spinel with an intermediate composition in the $ZnGa_2O_4$ - $ZnAl_2O_4$ system.

Various synthetic approaches, for example, the solid-state reaction as the most common route [7, 11, 17], flux method using Li_3PO_4 at high temperature [10, 23, 24], sol-gel method [25], low-temperature direct synthesis [26, 27], co-precipitation [9, 28], homogeneous precipitation [29], hydrothermal method [30, 31], and combustion synthesis [32] have been employed for the preparation of $ZnGa_2O_4$ spinel. On the other hand, there are many methods for the preparation of $ZnAl_2O_4$ spinel, e.g. solid-state reaction [33], co-precipitation [34], sol-gel [35, 36], and, template-assisted synthesis [37]. The glycothermal synthesis with post heating at 400 °C and catalytic properties of $ZnAl_2O_4$ and $ZnGa_2O_4$ spinels have also been reported [38]. Some spinel-type $ZnAl_2O_4$ particles have been synthesized based on

* Corresponding author: hirano@aitech.ac.jp

the hydrothermal synthesis routes [14, 15, 18, 39, 40]. Most of those hydrothermal $ZnAl_2O_4$ spinels have been prepared via the combination of post-heat-treatment at 500 ~ 800 °C in air. There are few reports concerning the synthesis via the hydrothermal route and the properties of spinel-type $ZnAlGaO_4$ nanocrystals at the intermediate composition between $ZnGa_2O_4$ and $ZnAl_2O_4$. Moreover the details of the effect of heating on the structure and properties of the as-prepared spinel nanocrystals have not yet been determined sufficiently.

In the present study, nanometer-sized $ZnAlGaO_4$ spinel solid solution particles have been hydrothermally synthesized using tetramethylammonium hydroxide, and their structure and properties, e.g. the cell size, optical band gap, and photoluminescence, have been investigated. In addition, a slight and gradual change in the cell size was observed in the as-prepared spinel nanoparticles during heating in air, the structural change of the $ZnAlGaO_4$ spinel in the course of hydrothermal treatment and post-heat treatment has been discussed.

II. Experimental

(1) Sample preparation

The nanocrystalline $ZnAlGaO_4$ spinel particles were prepared with the hydrothermal method at 150 ~ 240 °C for 5 h using tetramethylammonium hydroxide ($N(CH_3)_4OH$, TMAH). An aqueous solution mixture of reagent-grade $ZnSO_4$, $Al(NO_3)_3$ and $Ga(NO_3)_3$ in the ratios of Zn:Al:Ga = 1:1:1 was prepared in a Teflon container. Before hydrothermal treatment, $N(CH_3)_4OH$ solution was added into the solution mixture until the pH of the solution that was hydrothermally treated became weakly basic. This solution mixture with total cation concentrations (Zn + Al + Ga) of 0.20 mol/dm^3 in the Teflon container was then placed in a stainless steel vessel. The vessel was tightly sealed and it was heated at 150 ~ 240 °C for 5 h under rotation at 1.5 rpm. After hydrothermal treatment, the precipitates were washed with distilled water until the pH value of the rinsed water became 7.0, separated from the solution by means of centrifugation, and dried in an oven at 60 °C. The powders thus prepared under hydrothermal conditions at 180 °C were heat-treated in an alumina crucible at a heating rate of200 °C/h, held at 400 ~ 1000 °C for 1 h in air, and then cooled to room temperature in a furnace.

(2) Characterization

Phase identification of the as-prepared and heat-treated samples was conducted with an x-ray diffractometer (XRD, model: RINT-2000, Rigaku, Tokyo, Japan) using CuKα radiation. The morphology of the samples was observed using transmission electron microscopy (TEM, model: JEM-2010, JEOL, Tokyo, Japan). The crystallite size of the cubic spinel phase was evaluated from the line broadening of 311 diffraction peak, according to the Scherrer equation, $D_{XRD} = K\lambda/\beta\cos\theta$, where θ is the Bragg angle of diffraction lines; K is a shape factor (K = 0.9 in this work); λ is the wavelength of incident x-rays, and β is the corrected half-width given by $\beta^2 = \beta_m^2 - \beta_s^2$, where β_m is the measured half-width and β_s is the half-width of a standard sample. The peak-top positions of XRD patterns were measured using silicon as the internal standard. The specific surface area of the prepared samples was calculated from the adsorption isotherm of nitrogen at 77 K based on the Brunauer-Emmett-Teller method (BET, model: NOVA 1200, Yuasa Ionics, Osaka, Japan).

The UV-vis absorption (diffuse reflectance) spectra of the prepared powders were measured using an ultraviolet-visible spectrophotometer with an integrating sphere attachment (model: V-560, Nihon Bunko, Tokyo, Japan). The spectra were derived from the measured ones using the Kubelka-Munk equation [41]. The photoluminescence (PL) emission was measured using a fluorescence spectrophotometer (model: F-2700, Hitachi High-Tech, Japan) with a Xe lamp. Powder samples were excited with 270 nm radiation from a 150 W xenon lamp. The emission wavelength was scanned from 280 to 800 nm at a scanning rate of 60 nm/min.

III. Results and Discussion

(1) Synthesis of $ZnAlGaO_4$ spinel nanoparticles

The aqueous precursor solution (with composition: $ZnAlGaO_4$) was hydrothermally treated under weakly basic conditions using TMAH. There was no presence of unreacted metal cations in the ultrafiltrated solution after hydrothermal treatment under weakly basic conditions in all samples. The XRD patterns of as-prepared samples that were formed at 150 ~ 240 °C for 5 h are shown in Fig. 1. The precipitates formed at 150 ~ 240 °C were detected as a single phase corresponding to a spinel-type cubic structure, and no diffraction peaks due to another crystalline phase was detected. It was found that the crystalline products composed of a single phase of spinel-type cubic structure were obtained under hydrothermal conditions higher than 150 °C in the presence of TMAH.

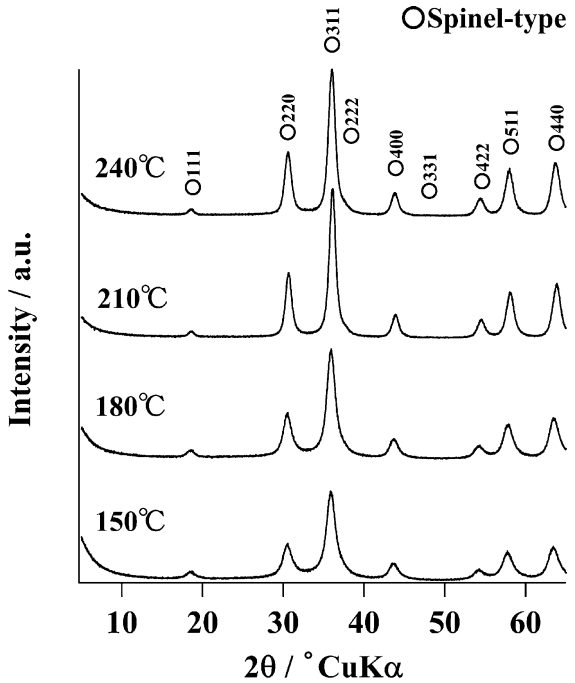

Fig. 1: X-ray diffraction patterns of precipitates obtained under hydrothermal conditions at 150 ~ 240 °C for 5 h.

The crystallite sizes of spinel-type cubic phase obtained after hydrothermal treatment at 150, 180, 210, and 240 °C, which were estimated from the line broadening of the 311 diffraction peak according to the Scherrer equation, were around 6, 8, 9, and 9 nm, respectively. The TEM images of precipitates formed at 150 and 210 °C are shown in Figs. 2(a) and (b), respectively. An increase in the particle size and crystallinity of spinel particles was seen as the treatment temperature rose. The particle sizes around 5 ~ 13 nm are observed for the precipitates obtained at 210 °C. As the crystallite size estimated from XRD line broadening corresponded relatively well to the particle size observed in TEM images, these particles are considered to be single crystals of spinel.

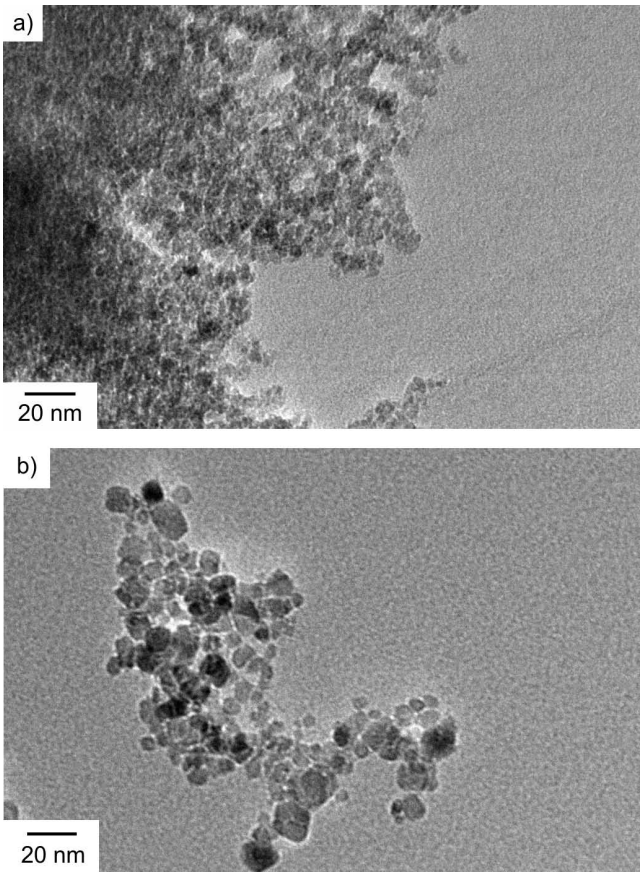

Fig. 2: Transmission electron microscopy images of precipitates obtained under hydrothermal conditions at (a) 150 and (b) 210 °C for 5 h.

Fig. 3 shows the detail of region around 58 and 65° 2θ, i.e. a shift of the cubic 511 and 440 lines in the XRD patterns of the precipitates formed at 150 ~ 240 °C, together with the XRD lines of the internal standard Si. It is found that the XRD lines of the cubic 511 and 440 of the spinel phase shift very slightly to a higher degree of 2θ, as the hydrothermal treatment temperature rises from 150 to 240 °C. Fig. 4 presents the change in the peak-top position (d_{440}) of cubic spinel phase prepared at 150 ~ 240 °C for 5 h. The interplanar spacing, d_{440} evaluated from the peak-top position of samples decreased very slightly and gradually with increased hydrothermal treatment temperature. Since the interplanar spacing of $ZnGa_2O_4$ and $ZnAl_2O_4$ is d_{440} = 0.1473 (JCPDS No. 38 – 1240) and d_{440} = 0.1429 nm (JCPDS No. 05 – 0669), respectively, the peak-top position (d_{440}) of samples approached the intermediate value of $ZnGa_2O_4$ and $ZnAl_2O_4$, i.e. the ideal value, little by little, as the hydrothermal treatment temperature rose from 150 to 240 °C. But the obtained values are larger than the ideal value. A gap exists between the peak-top position (d_{440}) of the as-prepared samples and ideal one. Then the as-prepared precipitates were heat-treated in air and are discussed in the next section.

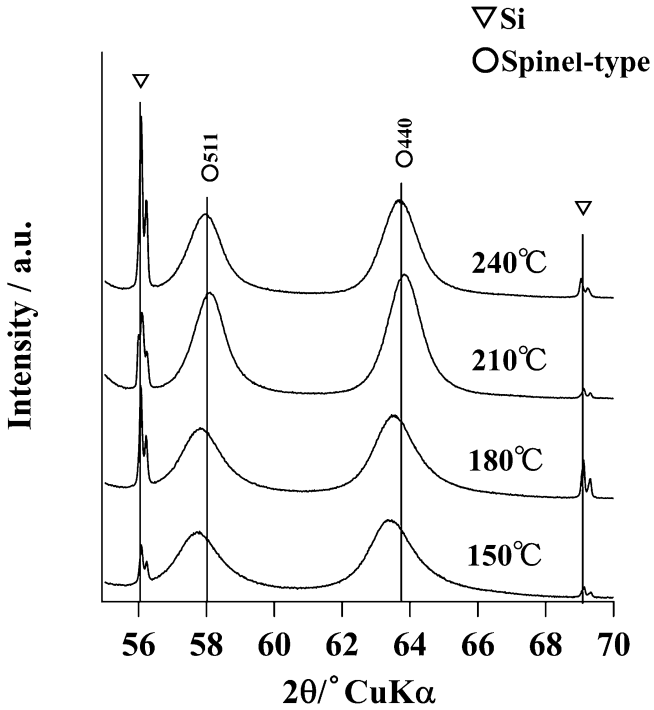

Fig. 3: Close-up of the region around 58 ~ 64° 2θ of the x-ray diffraction patterns of samples obtained under hydrothermal conditions at 150 ~ 240 °C for 5 h.

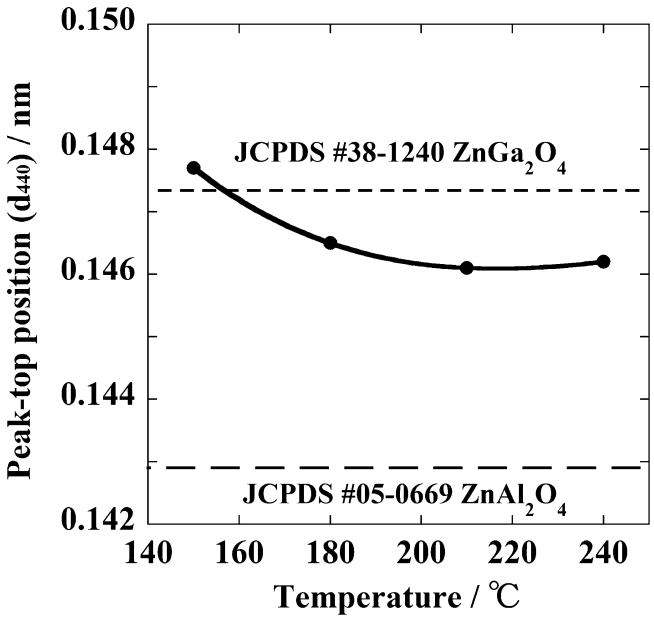

Fig. 4: Peak-top position (d_{440}) of cubic spinel phase of samples obtained under hydrothermal conditions at 150 ~ 240 °C for 5 h.

(2) Structural change through heat treatment

The effect of heat treatment in air on the crystallinity and structure of the as-prepared spinel nanoparticles was investigated. The precipitates with cubic spinel phase formed from the precursor solution with composition $ZnAlGaO_4$ under hydrothermal conditions at 180 °C were heat-treated at 400 °C ~ 1000 °C for 1 h in air. The XRD patterns of samples after heating in air at 400 °C ~ 1000 °C are shown in Fig. 5. The crystalline phase of the samples after heating in air at temperatures of 400 ~ 1000 °C was a single phase of cubic spinel structure. The change in the sharpness of the XRD patterns is hardly observed between the as-prepared sample and samples heat-treated at 400 ~ 600 °C. The XRD lines corresponding to spinel phase gradually become sharp as the heating temperature rises from 700 to 1000 °C. This result suggests that the improvement in the crystalliniy of the spinel phase occurs during heating at temperatures higher than 700 °C.

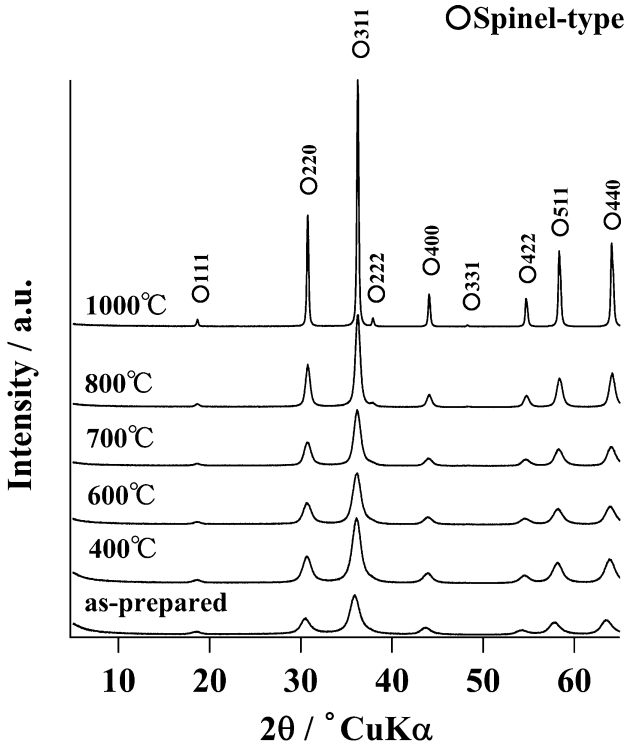

Fig. 5: X-ray diffraction patterns of samples hydrothermally formed at 180 °C before and after heating at 400 ~ 1000 °C for 1 h.

The TEM images of the samples after heating at 600 ~ 1000 °C are shown in Figs. 6 (a) ~ (c), respectively. The as-prepared nanocrystals with cubic spinel phase gradually grew to become large crystals as the heating temperature rose from 600 to 800 °C. The spinel crystals around 20 ~ 70 nm with cubic morphology are observed in the sample after heating at 1000 °C. The crystallite growth of spinel in the samples as a function of heating temperature is presented in Fig. 7. The crystallite size of the spinel hardly changed in the samples before and after heat treatment up to 600 °C for 1 h. The crystallite growth was accelerated by heating at temperatures higher than 800 °C. The resultant crystallite size of the spinel after heating at 1000 °C is around 45 nm, which corresponds relatively well to the average particle size estimated from the TEM observation in Fig. 6 (c). The BET surface areas of the spinel samples are plotted against the heating temperature in Fig. 8. The surface areas decreased almost linearly as the heating temperature rose.

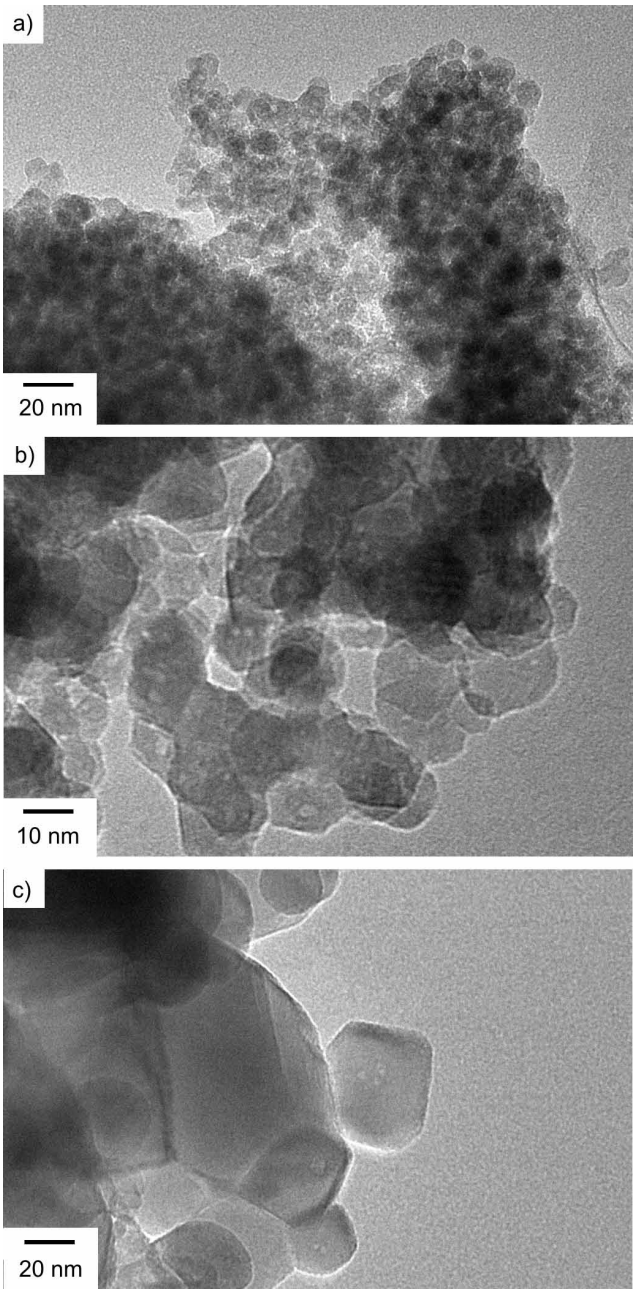

Fig. 6: Transmission electron microscopy images of samples heated at (a) 600, (b) 800, and (c) 1000 °C for 1 h.

Fig. 9 shows the detail of region around 58 and 65° 2θ, i.e. a shift of the cubic 511 and 440 lines in the XRD patterns of the samples as-prepared at 180 °C and heat-treated at 400 ~ 1000 °C, together with the XRD lines of the internal standard Si. It is observed that the XRD lines of the cubic 511 and 440 in the as-prepared spinel nanocrystals very slightly and gradually shift to higher degree of 2θ in accordance with heating at 400 ~ 800 °C. This phenomenon indicates that the as-prepared spinel nanocrystals undergo structural change as a result of the heat treatment.

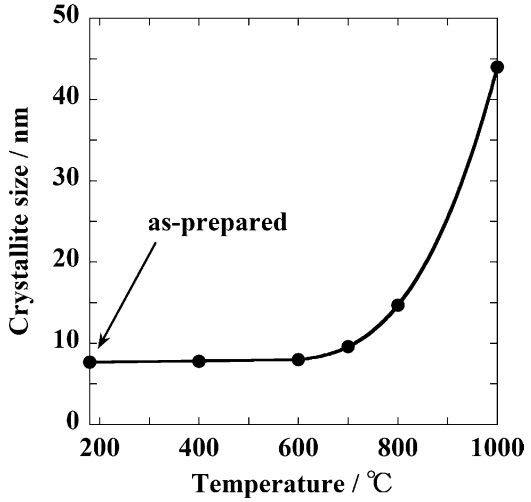

Fig. 7: Crystallite size of samples with cubic phase hydrothermally formed at 180 °C before and after heating at 400 ~ 1000 °C for 1 h.

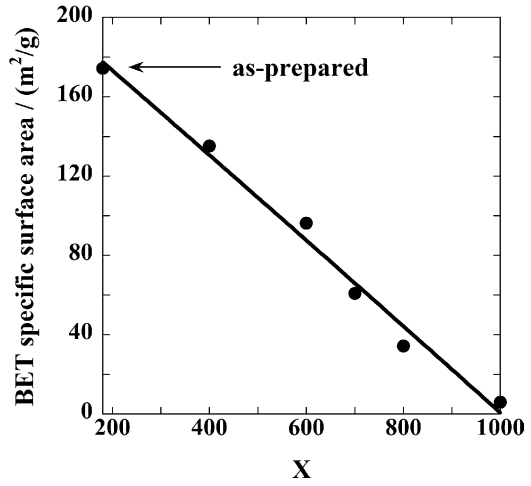

Fig. 8: BET specific surface area of samples hydrothermally formed at 180 °C before and after heating at 400 ~ 1000 °C for 1 h.

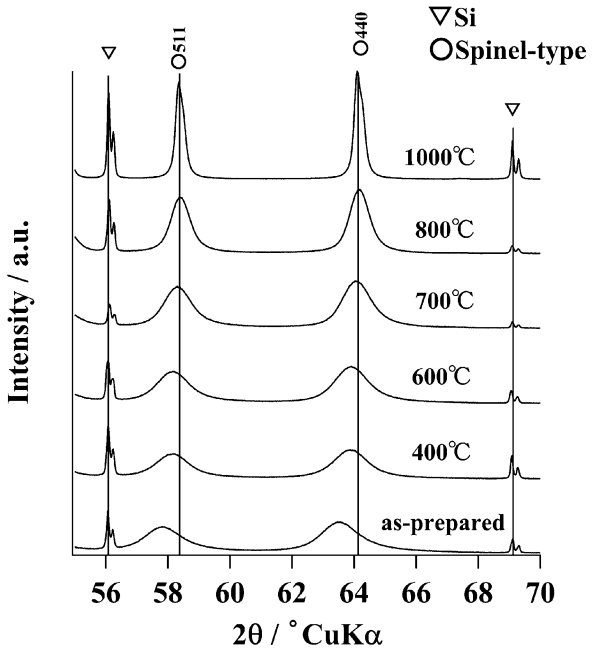

Fig. 9: Close-up of the region around 58 ~ 64 °; 2θ of the x-ray diffraction patterns of samples hydrothermally formed at 180 °C before and after heating at 400 ~ 1000 °C for 1 h.

The peak-top position (d_{440}) of the as-prepared spinel phase formed under hydrothermal condition at 180 °C and that after heat-treatment at 400 ~ 1000 °C are shown as a function of heating temperature in Fig. 10. The interplanar spacing, d_{440} evaluated from the peak-top position of the as-prepared cubic spinel phase slightly and linearly decreased as the heating temperature rose from 400 to 800 °C. After heating at temperatures higher than 800 °C, the interplanar spacing, d_{440} reached almost the constant value: 0.1451 nm. The cause of this phenomenon is considered to be as follows. The ideal value of d_{440} for $ZnAlGaO_4$ spinel solid solution estimated from the JCPDS data is around 0.1451 nm, which is an intermediate value between the d_{440} of $ZnAl_2O_4$ spinel: 0.1429 nm (JCPDS No. 05 – 669) and that of $ZnGa_2O_4$ spinel: 0.1473 nm (JCPDS No. 38 – 1240). Although it is not so easy to evaluate and discuss the cell size of the as-prepared spinel because the peaks are so broad, we have done this. The calculated value (d_{440}) for the as-prepared spinel formed under hydrothermal conditions at 180 °C from the precursor solution with composition $ZnAlGaO_4$ using XRD data is 0.1465 nm, which is slightly larger than that of the ideal value: 0.1451 nm. The peak-top position (d_{440}) of the as-prepared spinel which was located near that of $ZnGa_2O_4$ spinel: 0.1473 nm approached the intermediate ideal value of $ZnAlGaO_4$ spinel: 0.1451 nm with increased heating temperature. This result suggests that the possibility of the presence of spinel phase with low crystallinity or amorphous-like phase having a composition rich in Al in the as-prepared spinel nanocrystals in addition to the possibility of the presence of a small amount of OH^- species. The as-prepared state might be composed of Ga-rich $ZnAl_xGa_{1-x}O_4$ spinel phase and a small amount of Al-rich phase with low crystallinity or amorphous-like phase. As shown in Fig. 4, the cell size of the spinel phase gradually approached the ideal one of $ZnAlGaO_4$ as the hydrothermal treatment temperature rose.

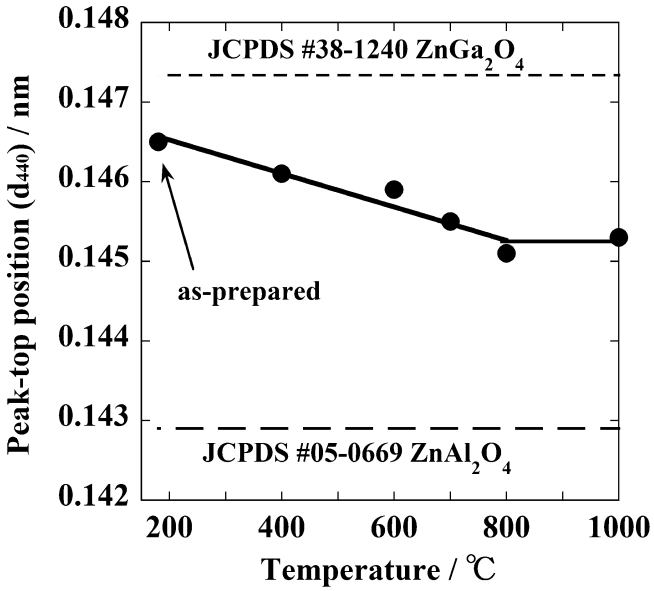

Fig. 10: Peak-top position (d_{440}) of cubic spinel phase of samples hydrothermally formed at 180 °C before and after heating at 400 ~ 1000 °C for 1 h.

In the course of heating up to 600 °C in air, a small amount of Al-rich phase with low crystallinity that is present in the as-prepared sample is considered to decrease as a result of the enhancement in crystallinity of spinel phase, which is the main reason why the surface area became smaller monotonically with the temperature (Fig. 8) although the crystallite sizes were almost constant up to 600 °C (Fig. 7). A substantial change in the cell size of the spinel phase after heating at temperatures higher than 800 °C could not be observed.

(3) Optical and luminescence properties

In the present study, the diffuse reflectance spectra of powder samples were measured using an ultraviolet-visible spectrophotometer with an integrating sphere attachment. The diffuse reflectance spectra and plots of transformed Kubelka-Munk function vs. the energy of light absorbed of the as-prepared $ZnAlGaO_4$ spinel and the spinel after heating at 800 and 1000 °C are shown in Fig. 11(a) and (b), respectively. The absorption edge of the samples changed slightly depending on the heat treatment. The optical band gap data obtained for the $ZnAlGaO_4$ spinel as-prepared and after heating at 800 and 1000 °C, which were evaluated based on the plots of transformed Kubelka-Munk function vs. the energy of light absorbed of samples (Fig. 11 (b)), are listed in Table 1.

Table 1: Optical band gap of $ZnAlGaO_4$ spinel.

Sample	Optical band gap (eV)
As-prepared	4.58
After heating at 800 °C	4.35
After heating at 1000 °C	4.53

There has been many investigations on the band gap of $ZnAl_2O_4$ and $ZnGa_2O_4$ spinel [42]. According to the results from the estimation on the band gap and structure, the $ZnAl_2O_4$ spinel possesses a larger band gap than $ZnGa_2O_4$ spinel. The band gap values of $ZnAl_2O_4$ spinel calculated using density functional theory (DFT) [43], the tight-binding muffin-tin orbital method (TB-LMTO) [44], GW approximation [43], and the modified Becke-Johnson potential (MBJ)[43] are 4.25, 4.11, 6.55, and 6.18 eV, respectively. On the other hand, the band gap values of $ZnGa_2O_4$ spinel estimated by means of DFT, TB-LMTO, GW, and MBJ are 2.82 [43], 2.79 [44], 4.57 [43], and 4.71 eV [43], respectively. The obtained band gap values for $ZnAlGaO_4$ spinel in this study are around 4.5 eV, which may be fairly reasonable. This result is supported by the report [45], in which the incorporation of aluminum ion into the $ZnGa_2O_4$ lattice results in the blue shifts of the absorption band of $ZnGa_2O_4$, bringing about the wider band gap. However, the band gap value of $ZnAlGaO_4$ spinel derived in this study are a little bit wider than those reported values based on the DFT and TB-LMTO method, on the one hand, and a little bit narrower than those based on the GW and MBJ method, on the other, according to the estimation as intermediate values between $ZnAl_2O_4$ and $ZnGa_2O_4$ spinel.

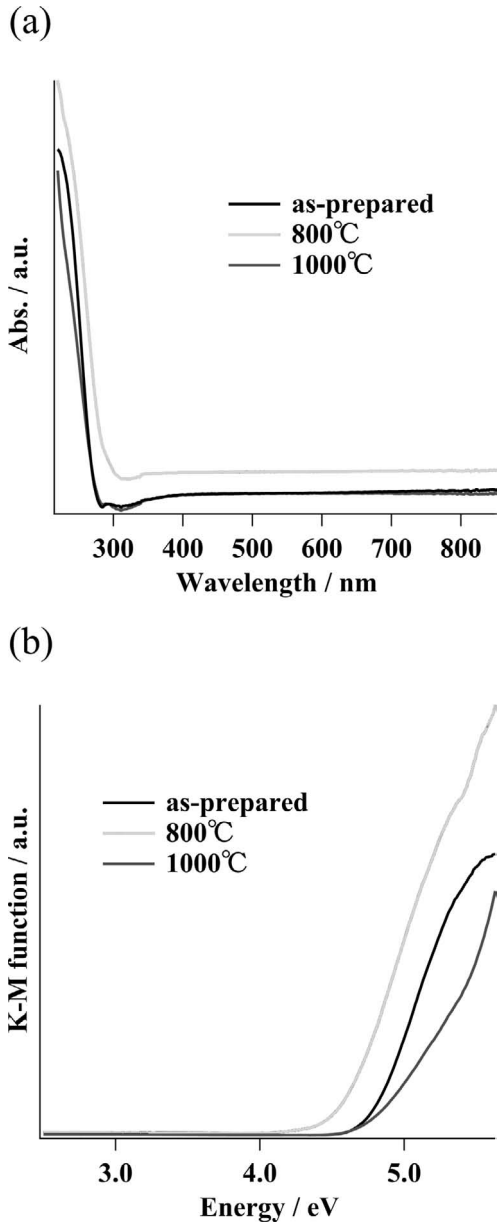

Fig. 11: (a) Diffuse reflectance spectra of samples hydrothermally formed at 180 °C before and after heating at 1000 °C for 1 h. (b) Plots of transformed Kubelka-Munk function vs. the energy of light absorbed of samples.

The room temperature photoluminescence spectra under excitation at 270 nm for the $ZnAlGaO_4$ spinel as-prepared and after heating at 800 and 1000 °C are shown in Fig. 12. The spectrum of the as-prepared spinel contains a wide band emission in the UV-blue region. The photoluminescence spectrum of the as-prepared spinel changed depending on the heat treatment. The center wavelength of the broadband UV-blue emission for the as-prepared sample was around 360 nm. On the other hand, the center wavelength of the broad band emission for the sample after heating at 800 °C was around 430 nm in the range of UV-blue~green. The spectrum of the spinel heated at 1000 °C seems to consist of more than two main broad band emissions with center wavelength at around 360 and 430 nm, and the emission intensity became low.

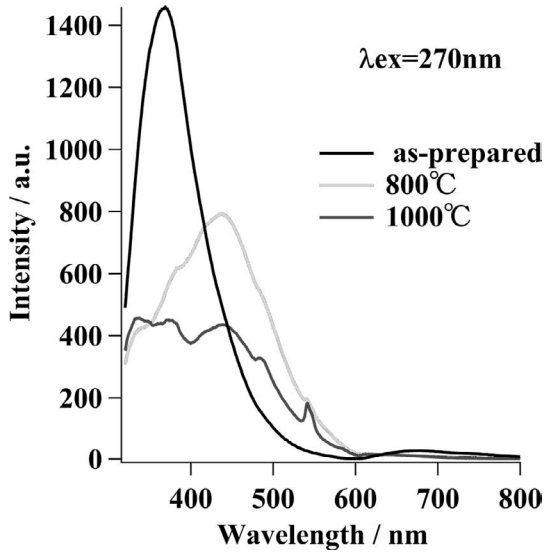

Fig. 12: Emission spectra of samples as-prepared at 180 °C and after heating at 800 and 1000 °C for 1 h. (λ_{ex} = 270 nm)

Concerning two main broad bands, a model in which the origin of 360 nm emission is the Ga-O transition at octahedral sites distorted owing to single oxygen vacancies (V_O^*) generation in $ZnGa_2O_4$, whereas 430 nm emission originates from the Ga-O transition of regular octahedral sites without V_O^* in $ZnGa_2O_4$ has been proposed [46]. The observed broad bands are assigned to the charge transfer between Ga^{3+} or Al^{3+} ions at octahedral sites and its surrounding O^{2-} ions [45]. These transitions may originate from the inter-band-gap defects, such as oxygen vacancies. These defects provide donor levels near the conduction band edge of the oxide according to the literature [8, 10, 47, 48] although the origins of the emissions of nano-sized oxides, e.g. spinel-type γ-Ga_2O_3 [49] and γ-Al_2O_3 [50] are still a matter of discussion.

IV. Summary

$ZnAlGaO_4$ spinel nanocrystals were formed via the hydrothermal route at 150 ~ 240 °C for 5 h in the presence of tetramethylammonium hydroxide. The structure, cell size, crystallite size, optical band gap, and luminescence of $ZnAlGaO_4$ spinel were investigated and discussed using as-prepared and post-heated samples. The cell size of as-prepared spinel phase changed slightly as the hydrothermal treatment temperature rose from 150 to 240 °C. The crystallite size of spinel obtained after hydrothermal treatment at 180 °C was around 8 nm. The crystallite growth was accelerated by heating at temperatures higher than 800 °C. The resultant crystallite size of the spinel after heating at 1000 °C was around 44 nm. The cell size of the as-prepared spinel decreased slightly and linearly as the heating temperature rose from 400 to 800 °C. After heating at temperatures higher than 800 °C, the cell size reached almost the constant of ideal value, which is intermediate value between the JCPDS data of $ZnAl_2O_4$ spinel and that of $ZnGa_2O_4$ spinel. The optical band gap of the $ZnAlGaO_4$ spinel was around 4.5 eV. The relatively high intensity of UV-visible blue light emissions centered at around 360 and 450 nm were obtained under excitation at 270 nm for $ZnAlGaO_4$ spinel as-prepared and that heat-treated at 800 °C, respectively.

References

1 Rao, C.N.R., Vivekchand, S.R.C., Biswasa, K., Govindaraja, A.: Synthesis of inorganic nanomaterials, *Dalton T.*, **34**, 3728 – 49, (2007).

2 Dawson, W.J.: Hydrothermal synthesis of advanced ceramic powders, *Am. Ceram. Soc. Bull.*, **67**, 1673 – 78, (1988).

3 Hirano, M., Morikawa, H., Inagaki, M., Toyoda, M.: Direct synthesis of new zircon-type $ZrGeO_4$ and Zr(Ge, Si)O_4 solid solutions, *J. Am. Ceram. Soc.*, **85**, 1915 – 20, (2002).

4 Hirano, M., Matsushima, K.: Photoactive and adsorptive niobium-doped anatase (TiO_2) nanoparticles: Influence of hydrothermal conditions on their morphology, structure, and properties, *J. Am. Ceram. Soc.*, **89**, 110 – 17, (2006).

5 Hirano, M., Dozono, H.: Luminescence nanocrystals in the rare-earth niobate-zirconia system formed via hydrothermal method, *J. Solid State Chem.*, **204**, 335 – 40, (2013).

6 Minami, T.: New n-type transparent conductive oxides, *MRS Bull.*, **25**, 38 – 44, (2000).

7 Omata, T., Ueda, N., Ueda, K., Kawazoe, H.: New ultraviolet-transport electroconductive oxide, $ZnGa_2O_4$ spinel, *Appl. Phys. Lett.*, **64**, 1077 – 78, (1994).

8 Shea, L.E., Datta, R.K., Brown, Jr., J.J., Photoluminescence of Mn^{2+}-activated $ZnGa_2O_4$, *J. Electrochem. Soc.*, **141**, 1950 – 54, (1994).

9 Kho, J.-G., Park, H.-D., Kim, D.-P.: Photoluminescence of the Mn-doped $ZnGa_2O_4$ phosphors prepared by coprecipitation of metals salts, *Bull. Korean. Chem. Soc.*, **20**, 1035 – 39, (1999).

10 Itoh, S., Toki, H., Sato, Y. Morimoto, K., Kishino, T.: The $ZnGa_2O_4$ phosphor for low-voltage blue cathodoluminescence, *J. Electrochem. Soc.*, **138**, 1509 – 12, (1991).

11 Tran, T.K., Park, W., Tomm, J.W., Wagner, B.K., Jacobsen, S.M., Summers, C.J., Yocom, P.N., McClelland, S.K.: Photoluminescence properties of $ZnGa_2O_4$:Mn powder phosphors, *J. Appl. Phys.*, **78**, 5691 – 95, (1995).

12 Minami, T., Kuroi, Y., Takata, S.: Preparation of $ZnGa_2O_4$: mn phosphor thin films as emitting lays for electroluminescent devices, *J. Vac. Sci. Technol. A*, **14**, 1736 – 40, (1996).

13 Zhang, X., Huang, J., Ding, K., Hou, Y., Wang, X., Fu, X.: Photocatalytic decomposition of benzene by porous nanocrystalline $ZnGa_2O_4$ with a high surface area, *Environ. Sci. Technol.*, **43**, 5947 – 51, (2009).

14 Chen, X.Y., Ma, C., Zhang, Z.J., Wang, B.N.: Ultrafine gahnite ($ZnAl_2O_4$) nanocrystals: hydrothermal synthesis and photoluminescent properties, *Mater. Res. Bull.*, **45**, 1889 – 93, (2010).

15 Mu, L., Wan, J., Wang, Z., Gao, Y., Qian, Y.: Mn-doped zinc aluminate nanoparticles: hydrothermal synthesis, characterization, and photoluminescence properties, *J. Nanosci. Nanotechno.*, **6**, 863 – 67, (2006).

16 Phani, A.R., Passacantando, M., Santucci, S.: Synthesis and characterization of zinc aluminum oxide thin films by sol-gel technique, *Mater. Chem. Phys.*, **68**, 66 – 71, (2001).

17 Sampsth, S.K., Cordaro, J.F.: Optical properties of zinc aluminate, zinc gallate, and zinc aluminogallate spinel, *J. Am. Ceram. Soc.*, **81**, 649 – 54, (1998).

18 Li, X., Zhu, Z., Zhao, Q., Wang, L.: Photocatalytic degradation of gaseous toluene over $ZnAlO_4$ prepared by different methods: A comparative study, *J. Hazard. Mater.*, **186**, 2089 – 96, (2011).

19 Shioyama, T.K.: Alcohol dehydration employing a zinc aluminate catalyst, U. S. Patent 4,260,845, (1981).

20 Aquilar-Rios, G., Valenzuela, M., Salas, P., Armendariz, H., Bosch, P., Del Toro, G., Sila, R., Bertin, V., Castillo, S., Schifter, A.I.: Hydrogen interactions and catalytic properties of platinum-tin supported on zinc aluminate, *Appl. Catal. A: General*, **127**, 65 – 75, (1995).

[21] El-Nabarany, T., Attia, A.A., Alayn, M.N.: Effect of thermal treatment on the structural, textural and catalytic properties of the ZnO-Al_2O_3 system, *Mater. Lett*., **24**, 319 – 25, (1995).

[22] Roesky, R., Weiguny, J., Bestgen, H., Dingerdissen, U.: An improved synthesis method for indenes and styrenes by use of a ZnO/Al_2O_3 spinel catalyst, *Appl. Catal. A: General*, **176**, 213 – 20, (1999).

[23] Yan, Z., Takei, H.: Flux growth of single crystals of spinel Zn-Ga_2O_4 and $CdGa_2O_4$, *J. Cryst. Growth*, **171**, 131 – 35, (1997).

[24] Yan, Z., Takei, H., Kawazoe, H.: Electrical conductivity in transparent $ZnGa_2O_4$: Reduction and surface-layer structure transformation, *J. Am. Ceram. Soc*., **81**, 180 – 86, (1998).

[25] Sei, T., Nomura, Y., Tsuchiya, T.: Preparation of $ZnGa_2O_4$ thin film by sol-gel process and effect of reduction on its electric conductivity, *J. Non-Cryst. Solids*, **218**, 135 – 38, (1997).

[26] Hirano, M., Okumura, S., Hasegawa, Y., Inagaki, M.: Direct precipitation of spinel type oxides $ZnGa_2O_4$ from aqueous solutions at low temperature below 90 °;C, *Int. J. Inorg. Mater*., **3**, 809 – 11, (2001).

[27] Hirano, M., Okumura, S., Hasegawa, Y., Inagaki, M.: Precipitation of spinel-type Zn(Fe, Ga)$_2O_4$ solid solutions from aqueous solutions below 90 °;C: Influence of iron valence of staring salt on their crystallite growth, *J. Solid State Chem*., **168**, 5 – 10, (2002).

[28] Zou, L., Xiang, X., Wei, M., Li, F., Evans, D.G.: Single-crystalline $ZnGa_2O_4$ spinel phosphor via a single-source inorganic precursor route, *Inorg. Chem*., **47**, 1361 – 69, (2008).

[29] Tas, A.C., Majewski, P.J., Aldinger, F.: Chemical synthesis of crystalline, pure or Mn-doped $ZnGa_2O_4$ powders at 90 °;C, *J. Mater. Res*., **17**, 1425 – 33, (2002).

[30] Hirano, M.: Hydrothermal synthesis and characterization of $ZnGa_2O_4$ spinel fine particles, *J. Mater. Chem*., **10**, 469 – 72, (2000).

[31] Hirano, M., Sakaida, N.: Hydrothermal synthesis and low temperature sintering of zinc gallate spinel fine particles, *J. Am. Ceram. Soc*., **85**, 1145 – 1150, (2002).

[32] Kim, J.Y., Kang, J.H., Lee, D.C., Jeon, D.Y.: Preparation and characterization of $ZnGa_2O_4$ phosphors synthesized with an optimized combustion process, *J. Vac. Soc. Technol.B*, **21**, 532 – 35, (2003).

[33] Hong, W.S., De, J.L., Yang, X., Rahaman, M.N.: Reaction sintering of ZnO-Al_2O_3, *J. Am. Ceram. Soc*., **78**, 3217 – 24, (1995).

[34] Huttig, G.F., Worl, H., Weitzer, H.H.: Reactions between solids. the formation of zinc aluminate from zinc oxide and aluminum oxide and the formation of copper-nickel alloys from mixtures of copper and nickel powders, *Z. Anorg. Allg. Chem*., **283**, 207 – 16, (1956).

[35] Kurihara, L.K., Suib, S.L.: Sol-gel synthesis of ternary metal oxides. 1. synthesis and characterization of MAl_2O_4 (M = Mg, Ni, Co, Cu, Fe, Zn, Mn, Cd, Ca, Hg, Sr, and Ba) and lead aluminum oxide ($Pb_2Al_2O_5$), *Chem. Mater*., **5**, 609 – 13, (1993).

[36] Mathur, S., Veith, M., Haas, M., Shen, H., Lecerf, N., Huch, V.: Single-source sol-gel synthesis of nanocrystalline $ZnAl_2O_4$: structural and optical properties, *J. Am. Ceram. Soc*., **84**, 1921 – 28, (2001).

[37] Wang, Y., Wu, K.: As a whole: crystalline zinc aluminate nanotube array nanonet, *J. Am, Chem. Soc*., **127**, 9686 – 87, (2005).

[38] Takeguchi, T., Kani, Y., Inoue, M., Eguchi, K.: Steam reforming of methanolon copper catalysts supported on large-surface area $ZnAl_2O_4$, *Catal. Lett*., **83**, 49 – 53, (2002).

[39] Zawadzki, M., Wrzyszcz, J.: Hydrothermal synthesis of nanoporous zinc aluminate with high surface area, *Mater. Res. Bull*., **35**, 109 – 14, (2000).

[40] Chen, Z., Shi, E., Zheng, Y., Li, W., Wu, N., Zhong, W.: Synthesis of mono-dispersed $ZnAl_2O_4$ powders under hydrothermal conditions, *Mater. Lett*., **56**, 601 – 605, (2002).

[41] Kubelka, P., Munk, F.: A paper on the optics of colour coatings, in german, *Zeits. f. Techn. Physik*. **12**, 593 – 601, (1931).

[42] Zhang, L., Ji, G.-F., Zhao, F., Gong, Z.-Z.: First-principles study of the structural, mechanical and electronic properties of ZnX_2O_4 (X=Al, Cr and Ga), *Chin. Phys. B*., **20**, 047102, (2011).

[43] Dixit, H., Tandon, N., Cottenier, S., Saniz, R., Lamoen, D., Partoens, B., Speybroecl, V.V., Waroquier, M.: Electronic structure and band gap of zinc spinel oxide beyond LDA: $ZnAl_2O_4$, $ZnGa_2O_4$ and $ZnIn_2O_4$, *New J. Phys*., **13**, 063002, (2011).

[44] Sampath, S.K., Kanhere, D.G., Pandey, R.: Electronic structure of spinel oxides: zinc aluminate and zinc gallate, *J. Phys. Cond. Matt*., **11**, 3635 – 44, (1999).

[45] Jeong, I.K., Park, H.L., Mho, S.I.: Two self-activated optical centers of blue emission in zinc gallate, *Solid State Commun*., **105**, 179 – 83, (1998).

[46] Kim, J.S., Kang, H.I., Kim, W.N., Kim, J.I., Choi, J.C., Park, H.L., Kim, G.C., Kim, T.W., Hwang, Y.H., Mho, S.I., Jung, M.-C., Han, M.: Color variation of $ZnGa_2O_4$ phosphor by reduction-oxidation processes, *Appl. Phys. Lett*., **82**, 2029 – 31, (2003).

[47] Bae, S.Y., Seo, H.W., Na, C.W., Park, J.: Synthesis of blue-light-emitting $ZnGa_2O_4$ nanowires using chemical vapor deposition, *Chem. Commun*, 1834 – 35, (2004).

[48] Da Silva, A.A., Goçalves, A.S., Davolos, M.R.: Characterization of nanosized $ZnAl_2O_4$ spinel synthesized by the sol-gel method, *J. Sol-Gel Sci Technol.*, **49**, 101 – 105, (2009).

[49] Wang, T., Radovanovic, P.V.: Size-dependent electron transfer and trapping in strongly luminescent colloidal gallium oxide nanocrystals, *J. Phys. Chem. C*., **115**, 18473 – 78, (2011).

[50] Anjiki, A., Uchino, T.: Visible photoluminescence from photoinduced molecular species in nanometer-sized oxides: Crystalline Al_2O_3 and amorphous SiO_2 nanoparticles, *J. Phys. Chem. C*., **116**, 15747 – 55, (2012).